

RESEARCH

Open Access



Design and development of metal-organic framework-based nanocomposite hydrogels for quantification of deferiprone in exhaled breath condensate

Reza Moharami¹, Zahra Karimzadeh², Jafar Soleymani¹, Vahid Jouyban-Gharamaleki³, Maryam Khoubnasabjafari^{4,5}, Elaheh Rahimpour^{1*} and Abolghasem Jouyban¹

Abstract

In this study, a novel fluorescence nanoprobe based on Materials of Institute Lavoisier (MIL-101) metal-organic frameworks embedding into the agarose hydrogel is fabricated using a hydrothermal technique. It uses for sensitive quantification of deferiprone in exhaled breath condensate (EBC) samples. The morphology and characterization of MIL-101/agarose nanocomposite hydrogel is studied by transmission electron microscopy, dynamic light scattering instrument, powder X-ray diffraction analysis, and Fourier transform infrared spectroscopy. The probe shows a reasonable fluorescence intensity quenching in the presence of deferiprone due to the interactions between iron centers in MIL-101 (Fe) and deferiprone, which likely form non-fluorescent complexes. The proposed nanoprobe demonstrates a linear calibration curve from 0.005 to 1.5 $\mu\text{g mL}^{-1}$ with a detection limit of 0.003 $\mu\text{g mL}^{-1}$. The intra- and inter-day precision of the reported method are 0.3% and 0.4% ($n=5$, deferiprone concentration = 1.0 $\mu\text{g mL}^{-1}$), respectively. This method demonstrates high sensitivity and specificity towards deferiprone in the EBC samples and also presents a sensing platform with simplicity, convenience, fast implementation, and cost-effective in medical monitoring.

Keywords Fluorescence nanoprobe, MIL-101 MOF, Nanocomposite hydrogel, Deferiprone, Exhaled breath condensate

*Correspondence:

Elaheh Rahimpour

rahimpour_e@yahoo.com

¹Pharmaceutical Analysis Research Center, Faculty of Pharmacy, Tabriz University of Medical Sciences, Tabriz, Iran

²Research Center for Pharmaceutical Nanotechnology, Biomedicine Institute, Tabriz University of Medical Sciences, Tabriz, Iran

³Liver and Gastrointestinal Diseases Research Center, Tabriz University of Medical Science, Tabriz, Iran

⁴Tuberculosis and Lung Diseases Research Center, Tabriz University of Medical Science, Tabriz, Iran

⁵Department of Anesthesiology and Intensive Care, Faculty of Medicine, Tabriz University of Medical Sciences, Tabriz, Iran



© The Author(s) 2024. **Open Access** This article is licensed under a Creative Commons Attribution-NonCommercial-NoDerivatives 4.0 International License, which permits any non-commercial use, sharing, distribution and reproduction in any medium or format, as long as you give appropriate credit to the original author(s) and the source, provide a link to the Creative Commons licence, and indicate if you modified the licensed material. You do not have permission under this licence to share adapted material derived from this article or parts of it. The images or other third party material in this article are included in the article's Creative Commons licence, unless indicated otherwise in a credit line to the material. If material is not included in the article's Creative Commons licence and your intended use is not permitted by statutory regulation or exceeds the permitted use, you will need to obtain permission directly from the copyright holder. To view a copy of this licence, visit <http://creativecommons.org/licenses/by-nc-nd/4.0/>.

Introduction

Deferiprone as an orally active iron chelator was developed as a new therapy for iron overload. It is used globally to treat various diseases, including cancer, leukemia, and hemodialysis [1]. Patients who are being treated with deferiprone may experience some adverse effects including neutropenia/agranulocytosis, gastrointestinal problems, raised alanine amino transferase levels, and zinc deficiency. Deferiprone reacts with ferric ions to create 1:3 iron-deferiprone complexes that are neutral and hydrophilic [2]. Monitoring patients with liver or kidney problems is vital when administering medication with deferiprone. Measuring the drug levels in the blood or other body fluids is essential to determine the optimal dosage and frequency of administration, enhancing the effectiveness of the treatment while minimizing the risk of side effects [3]. Several quantitative analytical techniques have been developed for the determination of deferiprone, including capillary electrophoresis-frontal analysis [4], electrochemical [5, 6], reverse phase-high performance liquid chromatography with a UV detector (RP-HPLC) [7, 8], and spectroscopy [9] procedures. Chromatographic techniques are time-consuming processes and require lengthy sample preparation steps and the use of high-cost reagents. Additionally, electrochemical methods often exhibit limited reproducibility, which can hinder the development of new methods. Although these developed methods have their advantages and disadvantages, developing a new and easy-to-use method for drug concentration measuring in complex biological samples is a challenging issue for researchers. In contrast to other methods, optical-based methods are rapid and straightforward to operate, making them suitable for deployment in remote areas, but they lack sufficient selectivity and sensitivity. To enhance the selectivity and sensitivity of optical methods, the implementation of reliable platforms [10] or advanced computational processing techniques [11, 12] is crucial. In this regard, metal-organic frameworks (MOFs) are crystalline frameworks with high porosity, created by assembling inorganic metal-based nodes or clusters with organic ligands through strong coordination bonds [13]. The diverse array of metal ions, organic linkers, and structural motifs enables an almost limitless number of potential combinations. Additionally, the ability to modify structures after synthesis introduces an extra layer of complexity. When combined with the rapidly growing library of experimentally determined structures, it becomes feasible to accurately predict, using computational methods, the affinity of guests for host frameworks. This has significant implications for designing frameworks that can deliver specific properties [14]. The large specific surface area, considerable thermal and chemical stabilities, manageable compositions, and uniform pore size distribution are some

of the superior properties of MOFs [15]. These aspects have made MOFs ideal candidates for various applications [16–18]. The Materials Institute Lavoisier's (MILs) MOFs are a well-known class of materials characterized by their outstanding stability, permanent porosity, and extensive specific surface area [19]. Second-generation MOFs, exemplified by MILs, are formed via the combination of phthalic acid or terephthalic acid with trivalent metal ions like (Cr^{3+} , Fe^{3+} , Al^{3+} , etc.). These materials are known for their suitable thermal and chemical stability and many uncoordinated transition metal sites. MIL-101 serves as a prototypical representative of the MIL series, whose versatility allows for the incorporation of various functional groups to enhance its selectivity [20]. For instance, MOFs have the potential to be combined with various materials such as metal nanoparticles, polymers, graphene, and carbon nanotubes to produce various composites that possess unique functionality not present in pure MOF. Recent advances in MOF-polymer composites have led to the development of a new generation of materials with expanded practical applications, featuring desirable properties such as improved processability, electrical conductivity, molecular recognition capabilities, chemical and colloidal stability, and biocompatibility [21]. Recent research has focused on the development of MOF-based hydrogels, which have shown significant improvements over traditional MOFs in terms of mechanical strength, absorption capacity, and total pore volume [22]. Hydrogels are polymeric materials that can absorb and retain a significant amount of water without dissolving [23]. Hydrogels are being extensively researched for their superior softness, wetness, responsiveness, biocompatibility, and bioactivity. Agarose is a type of natural hydrogel derived from a polysaccharide found in the cell walls of marine red algae. Agarose can form a gel by aggregating its hexagonal fibers, which consist of six double helices, and absorbing a large amount of water within its network. Due to its hydrophilic polymeric framework, chemical stability, and tunable pore size, this material has become a popular choice as a supporting medium for optical sensors [24].

The objective of this study was to develop a sensing platform for determining deferiprone levels in exhaled breath condensate (EBC) by leveraging the unique properties of MIL-101/agarose nanocomposite hydrogels (NCH). Cooling-down strategy was utilized to synthesize MIL-101/agarose NCH to achieve the desired structure, stability, and morphology. Herein, agarose as the polymeric matrix, MIL-101 (Fe) as nanofiller, and reinforcement of hydrogel were employed. Deferiprone was selected as a representative analyte due to its wide range of therapeutic applications. In a subsequent step, the probe was used to investigate its ability to detect deferiprone in the EBC of patients undergoing treatment with

this medication (Fig. 1). The uniqueness of the method lies in its sustainable and biocompatible materials, ease of synthesis, and rapid detection capabilities, making it an innovative solution for sensing deferiprone in EBC.

Materials and methods

Reagents and solutions

Chemicals were obtained from commercial sources. The chemical and solvents, including N, N-dimethylformamide (DMF), terephthalic acid (H_2BDC , M_w :166.13 $g\ mol^{-1}$) and agarose NCH were purchased from Sigma-Aldrich (www.sigmaaldrich.com). Sodium dihydrogen phosphate (NaH_2PO_4) with an M_w of 119.98 $g\ mol^{-1}$ was utilized for buffer preparation. The pH of the buffer was adjusted to various levels using sodium hydroxide (NaOH) and hydrochloric acid (HCl) also $FeCl_3 \cdot 6H_2O$ and ethanol (EtOH) for the synthesis of MIL-101 (Fe) were supplied from Merck (www.merck.com). Deferiprone (> 99.7%) was achieved from Arastoo Pharmaceutical Co. (Tehran, Iran) and ultrapure deionized water from (Ghazi Pharmaceutical Co., Tabriz, Iran, www.sgco-infusion.com) was used for the dilution process. All reagents were stored at 4 °C before usage.

Apparatus and characterization

The fluorescence spectra were recorded using an FP-750 spectrofluorometer (Jasco Corp., Japan) with a xenon lamp source. A 1 mL standard quartz cell was used for all fluorescence spectra measurements, with a bandwidth

of 10 nm set in the excitation and 20 nm in emission paths. The distribution of particle size in the prepared nanoprobe was estimated and their shape and size were evaluated using a CM120 transmission electron microscopy (TEM) and dynamic light scattering (DLS) (Philips, The Netherlands, www.philips.com). The prepared solutions' UV-vis absorption spectra were recorded on a spectrophotometer model UV-1800 using a micro quartz cell (Shimadzu, Japan, www.shimadzu.com). Powder X-ray diffraction (XRD) patterns were obtained using a Siemens diffractometer with filtered $Cu-K\alpha$ radiation at 35 kV within the 2θ range 4° - 70° . Fourier transforms infrared (FT-IR) spectroscopy was used to verify the chemical bonding of the samples. The spectral width was set at 400 – $4000\ cm^{-1}$, and the instrument used was Bruker Tensor 27 (KBr wafer technique). MIL-101 (Fe) was successfully synthesized using an oven (Initiator 8 EXP, 2450 MHz frequency, Biotage Corp). The pH was adjusted using a model 744 digital pH meter (Metrohm Ltd., Switzerland).

Synthesis of MIL-101 (fe)

MIL-101 (Fe) was synthesized via hydrothermal synthesis, as described in [25]. First, 1.351 g of $FeCl_3 \cdot 6H_2O$ (5 mmol) and 0.415 g (2.5 mmol) of H_2BDC were mixed in 30 mL of DMF. The mixture was fully suspended by sonication for 20 min. Next, the suspension was placed in a Teflon-lined stainless-steel autoclave, sealed, and heated at 110 °C for 24 h. Then, the obtained solution

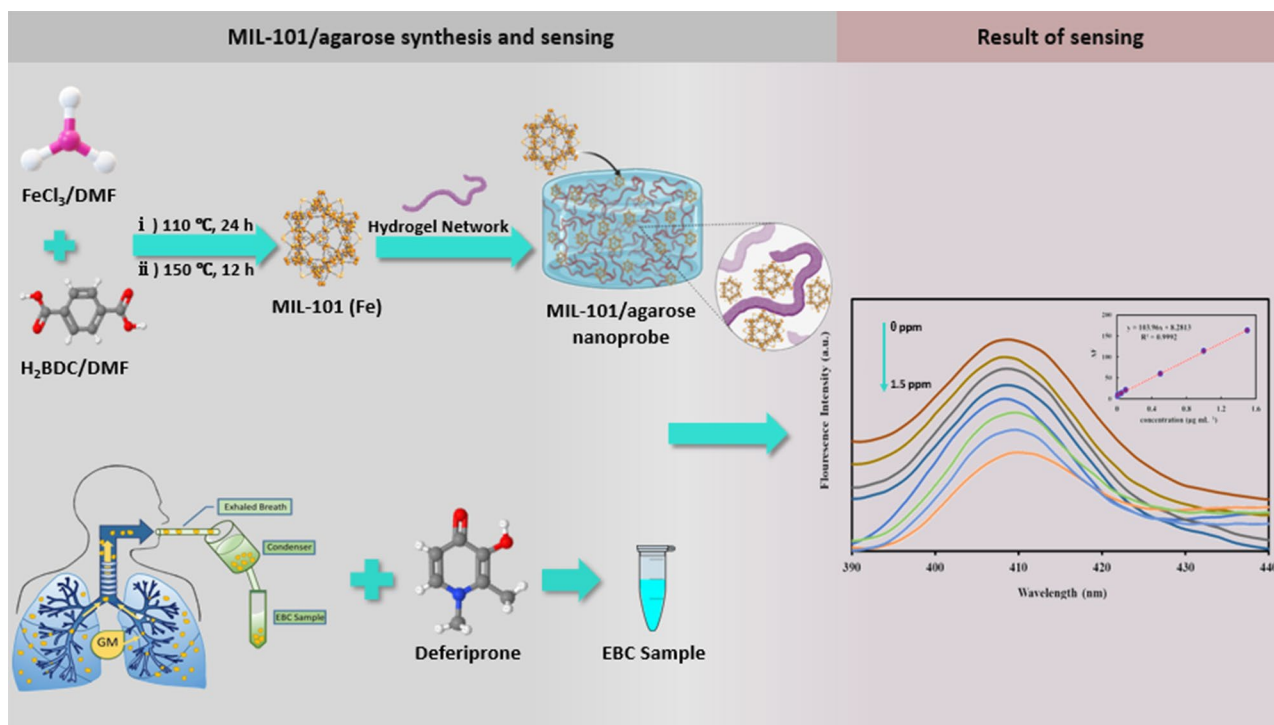


Fig. 1 A schematic illustration of MIL-101/agarose NCH synthesis and its application for deferiprone determination

was centrifuged, and the precipitated orange mud was washed three times with DMF and hot EtOH to remove the raw materials. The orange mud was dried at 70 °C for 60 min and then activated at 150 °C for 12 h.

Synthesis of MIL-101/agarose NCH

To prepare the MIL-101/agarose NCH according to other MOF and hydrogel composite [26], first, 0.0334 g of agarose was dissolved in 50 mL of water with a stirrer until fully dissolved at 80 °C. In the next part, 2.5 mg of synthesized MIL-101 was dispersed in 1 mL of deionized water and sonicated for 10 min. Then, 668 μL of the pre-prepared MIL-101 solution was added to the hot agarose solution and stirred for another 10 min at 90 °C to ensure homogeneity. The solution was cooled to room temperature to form MIL-101/agarose NCH. The obtained hydrogel was kept at 4 °C for further experiments.

Samples preparation

To prepare working standard solutions, our stock solutions were diluted daily with deionized water. To collect human EBC samples, we employed an exhalation collection device [27]. The EBC device featured a cooling trap with an adjustable temperature ranging from 0 °C to -25 °C. The cooling trap rapidly cooled the blown air and then removed the vaporized particles from the surface of the trap through condensed water vapor particles. The EBC samples were analyzed directly, without any prior preparation steps. The samples used for optimization and calibration methods were collected from healthy volunteers. Additionally, real samples were collected from four patients receiving deferiprone to check the method's applicability. The sample donors signed a consent form confirmed by the ethics committee of Tabriz University of Medical Sciences, with the code IR.TBZMED.PHARMACY.REC.1402.050.

General procedure

The fluorescence detection was done in a 2 mL vial using a batch procedure. For optimal conditions, 150 μL of EBC was added to the microtube and 10 μL of 0.1 mol L⁻¹ phosphate buffer (pH 4.0). Then, 20 μL of MIL-101/agarose NCH was added, and the final volume was adjusted to 0.5 mL using deionized water. The fluorescence intensity of the nanoprobe signal was measured immediately at around $\lambda_{\text{max}}=410$ nm after excitation at 360 nm. The analytical signal was quantified as ΔF , where ΔF is the difference between the probe intensity in the presence (F) and absence (F_0) of deferiprone. The experiments were conducted at room temperature.

Results and discussions

Structural characterization of MIL-101/agarose NCH

TEM was employed to investigate the morphology and particle size of MIL-101/agarose NCH. As depicted in Fig. 2A, MIL-101 (Fe) was dispersed well throughout the agarose matrix without aggregation and showed an intact crystal morphology with a size of lower than 200 nm. Zeta potential measurements in Fig. 2B indicated a negative zeta potential of -21.5 mV for MIL-101/agarose NCH. The negative zeta potential observed in the MIL-101/agarose NCH is mainly due to deprotonated carboxylate groups in the MIL-101 (Fe) structure. Additionally, the hydroxyl groups in the agarose component may play a role in increasing the negative surface charge. The combination of functional groups from the MOF structure and agarose molecules leads to the overall negative zeta potential observed in the NCH.

To further verify the successful synthesis of MIL-101/agarose NCH, FT-IR spectroscopy was conducted (Fig. 3A). For as-prepared MIL-101 (Fe), the absorption band at around 747, 1017, 1393, 1507 and 1600 cm⁻¹ belong to C-H bending vibrations in benzene, symmetric vibration of the carboxyl group (-COO-), asymmetric

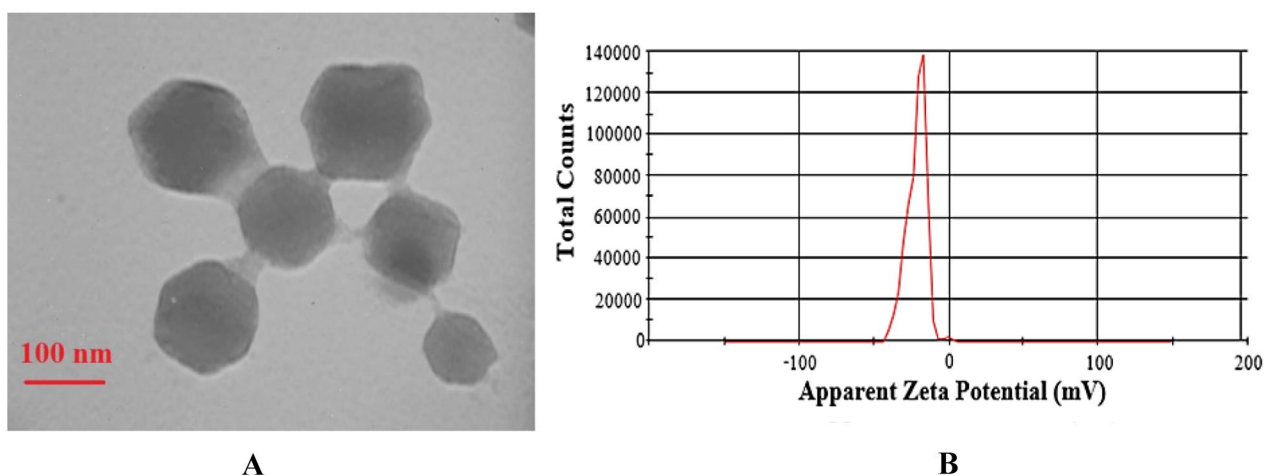


Fig. 2 (A) TEM image, and (B) zeta potential of MIL-101/agarose NCH

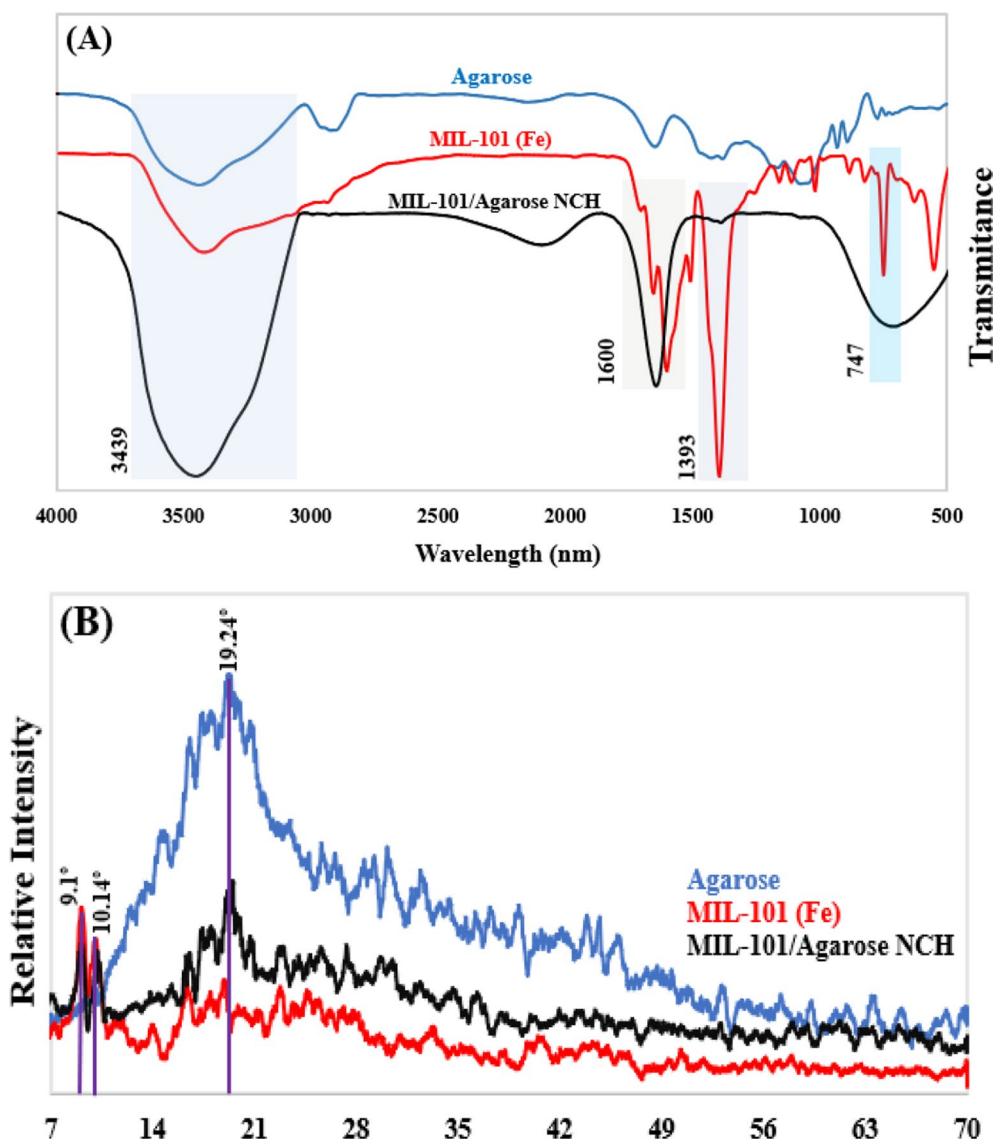


Fig. 3 (A) FT-IR spectra and (B) XRD patterns of Agarose, MIL-101 (Fe), and MIL-101/agarose NCH

vibration of the carboxyl group ($-\text{COO}-$), $\text{C}=\text{O}$ bonds in free carboxylic groups, respectively [28]. The C-H bending vibrations in benzene are indicated by the peak at 747 cm^{-1} . Symmetric and asymmetric vibrations of carboxyl groups ($-\text{COO}-$) are assigned to peaks at 1393 and 1507 cm^{-1} , respectively, while the peak at 1600 cm^{-1} is related to $\text{C}=\text{O}$ bonds in free carboxylic groups, demonstrating the dicarboxylate linker. These FT-IR peaks confirm the organic carboxylate bridging ligand structure and prove that the orange powder is crystal pure MIL-101 (Fe) [25]. The FT-IR spectra of agarose reveals specific absorption peaks at 3439 cm^{-1} (OH stretching of the hydroxyl group), 1646 cm^{-1} ($\text{C}=\text{O}$ stretching vibration), 1073 cm^{-1} (C-O glycosidic bonding), and 930 cm^{-1} (vibration of C-O-C bridge of 3, 6-anhydro-L-galactopyranose) [29]. In the case of MIL-101/agarose NCH,

similar bands with MIL-101 (Fe) and agarose with slightly different positions and intensities are shown, indicating the successful incorporation of MIL-101 (Fe) into the agarose matrix. Also, XRD analysis was performed on the samples to verify the crystallinity and phase purity of the materials (Fig. 3B). The typical characterization peaks of MIL-101 (Fe) can be seen at 9.1° and 10.14° related to (311) and (511) crystal planes at reasonably high intensity similar to that observed in previous studies [30]. Pure agarose shows a single peak at $2\theta = 19.24^\circ$ [31]. By comparing the XRD patterns of MIL-101/agarose NCH with MIL-101 (Fe) and agarose alone, the appearance of the peaks as mentioned earlier evidenced the successful fabrication of the MIL-101/agarose NCH.

Sensing mechanism

The performance of the synthesized nanoprobe has been analyzed after ensuring the preparation process. The interaction between the nanoprobe and deferiprone has been distinguished by studying the spectra and analytical response of the nanoprobe. A quenching process was observed in the fluorescence intensity of MIL-101/agarose NCH system after deferiprone adding, which can be attributed to the interactions between iron centers in MIL-101 (Fe) and deferiprone. These interactions are (i) coordination bonds: MIL-101 contains metal centers (chromium ions) that can form coordination bonds with functional groups on deferiprone, such as oxygen atoms from hydroxyl groups (-OH) or nitrogen atoms from the pyridine ring in deferiprone. (ii) hydrogen bonding: Hydrogen bonding can occur between hydroxyl groups (-OH) or nitrogen atoms in deferiprone and hydrogen bond acceptor sites on the MOF, such as hydroxyl or carbonyl groups on the terephthalate ligands and (iii) electrostatic interactions: Deferiprone contains ionizable groups, and MIL-101 may have charged sites or surface charges that can engage in electrostatic interactions with these groups. The interactions may have resulted in the creation of non-fluorescent complexes that do not exhibit fluorescence when excited, thereby reducing the observed fluorescence intensity [32]. The porous structure of MIL-101 (Fe) supports these interactions by facilitating the diffusion of deferiprone into the framework where it can directly interact with iron centers. The embedding in agarose does not impede this interaction but rather contributes to a controlled environment where deferiprone can efficiently access the MIL-101 (Fe) pores. This structural arrangement ensures that the quenching mechanisms are not merely surface phenomena but are deeply integrated into the material's framework, enhancing the sensitivity and specificity of the system towards deferiprone. The fluorescence signal of the proposed probe decreases in a concentration-dependent manner as deferiprone concentration increases, rendering it a valuable tool for the determination of deferiprone in various matrices.

Optimization of reaction conditions

Optimizing experimental conditions is crucial for probe design as it directly affects method performance. In the early stages of our study, we discovered that three variables (pH, MIL-101/agarose NCH concentration, and incubation time) had a significant impact on the fluorescent intensity. A deferiprone concentration of $1 \mu\text{g mL}^{-1}$ was set as the target value for the optimization protocol. The pH of the reaction environment plays a crucial role in modulating the complexation reactions between metal ions and ligands [33]. The effect of pH values was investigated on the system's response using phosphate buffer

(PBS, 0.10 mol.L^{-1}) ranging from 2.0 to 8.0. As the pH increased, the nanoprobe's response exhibited a marked enhancement, peaking at pH 4.0, where the highest fluorescence response (ΔF) was observed, and subsequently decreasing in higher pH values, as shown in Fig. 4A. The maximum fluorescence response was achieved at pH 4.0, likely due to the strong interaction between the deferiprone's N-containing group and the negative surface of nanoparticles, due to the pK_a value of deferiprone [34]. The optimal amount of MIL-101/agarose NCH was identified by varying the amount used in the design process and evaluating its impact on the system. It was observed that the highest fluorescence response of the nanoprobe was obtained at $20.0 \mu\text{L}$ of MIL-101/agarose NCH. Thus $20.0 \mu\text{L}$ was selected as the optimal volume, as illustrated in Fig. 4B. The decreasing in fluorescence after this value can be related to probe self-quenching at high concentration. The time taken for the reaction of deferiprone molecules and MIL-101/agarose NCH to reach equilibrium is called the incubation time. For this purpose, MIL-101/agarose NCH was added to a solution containing deferiprone and PBS (pH 4.0) for various periods. As the incubation time increased from 1 to 20 min, the response of the nanoprobe showed a decreasing pattern (Fig. 4C). So, fluorescence intensity was recorded immediately after solution preparation. The obtained optimal conditions for executing the reactions are as follows: pH:4.0, MIL-101/agarose concentration: $20 \mu\text{L}$, and incubation time: immediately.

Interference study with coexisting substances

The established fluorescent method needs to be investigated for its specificity and selectivity to study the effect of any potential interference caused by co-administered drugs with deferiprone. To evaluate selectivity, system responses towards potential available interfering substances including losartan, dexamethasone, amoxicillin, ampicillin, alprazolam, glucose, ibuprofen, clonazepam, phenytoin, carbamazepine, phenobarbital, acetaminophen, nicotinamide, caffeine, ascorbic acid, diclofenac, chlordiazepoxide, metoprolol, dextromethorphan, cetirizine, metronidazole, aspirin, and FeCl_3 were assessed in EBC media. The system response was tested using deferiprone and a range of interfering substances at a concentration of $1.0 \mu\text{g mL}^{-1}$. As shown in Fig. 5, the interferences had a negligible effect on the probe response. Therefore, it is suggested that this method could be best performed for deferiprone tracing in the EBC of patients receiving these drugs.

Analytical figures of merit

The optimal conditions were employed for the partial validation of the method in accordance with the guidelines set forth by the Food and Drug Administration

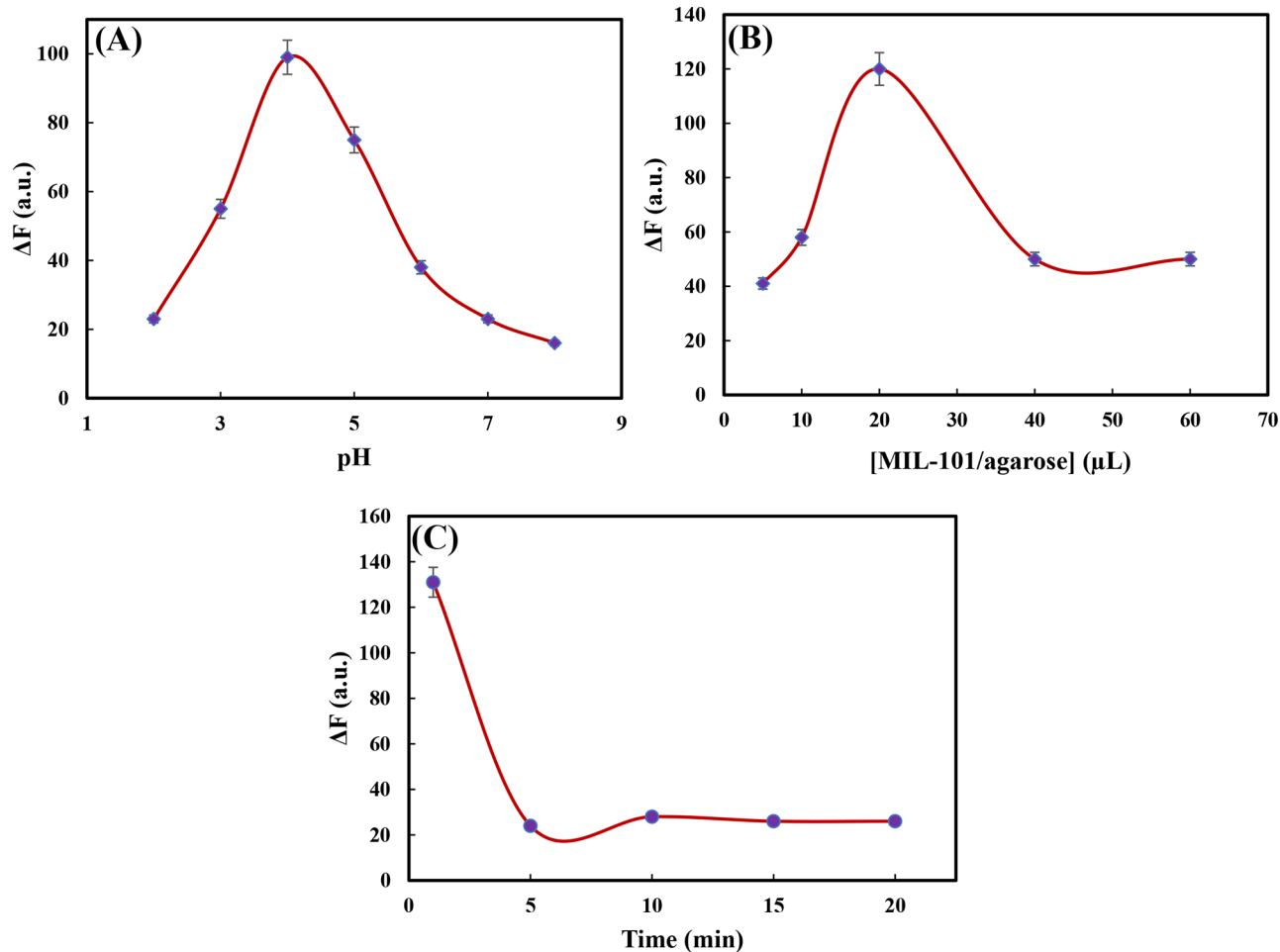


Fig. 4 Effect of (A) pH, (B) amount of MIL-101/agarose NCH, and (C) incubation time on the response of the system

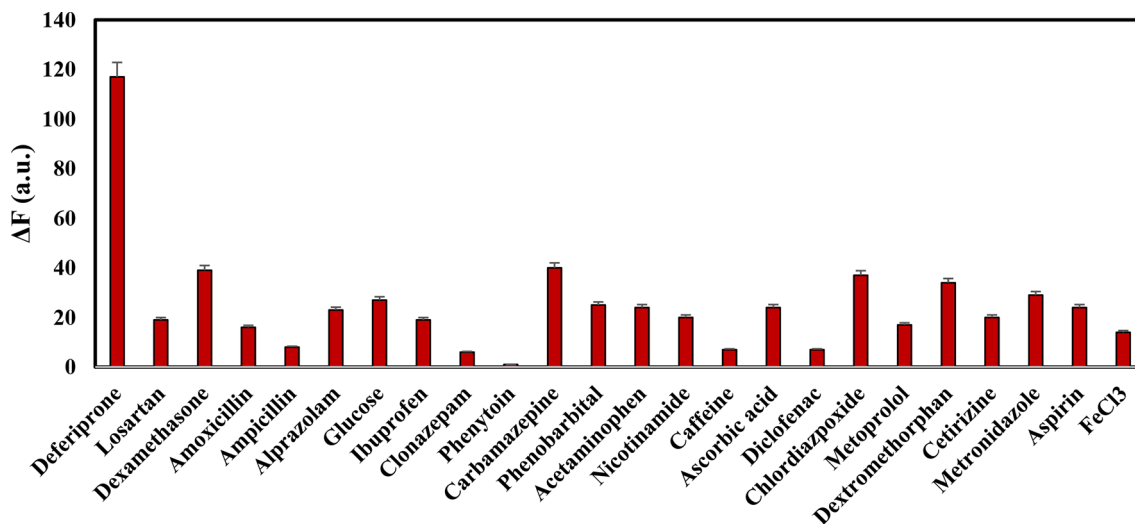


Fig. 5 Study of the method selectivity under optimal conditions (pH: 4 and 20 μL of nanoprobe) in the presence of some possible interfering drugs in EBC samples with concentrations of $1 \mu\text{g mL}^{-1}$

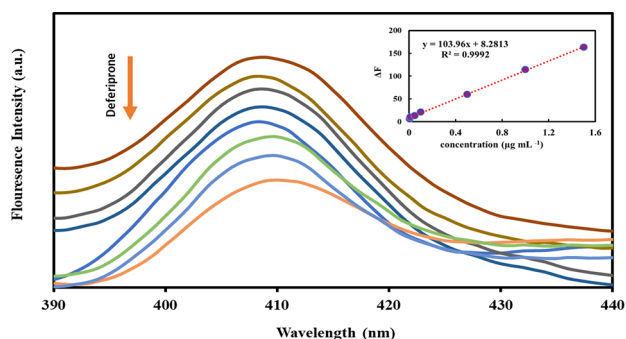


Fig. 6 Fluorescence intensity of MIL-101/agarose NCH in the absence and presence of deferiprone in the range of 0.005–1.5 $\mu\text{g mL}^{-1}$. Inset: Calibration curve obtained for deferiprone in EBC

Table 1 Determination of deferiprone in spiked EBC samples

Added ($\mu\text{g mL}^{-1}$)	Found \pm SD ($\mu\text{g mL}^{-1}$)	Recovery (%) ^a	t-test ^b
0.01	0.0098 \pm 0.007	98.0	0.05
0.50	0.52 \pm 0.03	104.0	1.2
1.00	1.03 \pm 0.02	103.0	2.6

^a Mean of three determinations \pm standard deviation

^b t-critical = 4.3 for $n=3$ and $P=0.05$

(FDA). First, the concentration-dependent behavior of the method was obtained in the optimum conditions. Figure 6 illustrates the fluorescence spectra of MIL-101/agarose NCH, which exhibits a peak at 410 nm upon excitation at 360 nm, and this peak intensity decreases as the deferiprone concentration is increased. The results indicated a linear relationship between the intensity and deferiprone concentration within the range of 0.005–1.5 $\mu\text{g mL}^{-1}$, as shown in the inset of Fig. 6. The equation for regression was $\Delta F (F - F_0) = 103.96 C_{DEF} + 8.2813$ ($R^2 = 0.9992$). In this equation, C_{DEF} represents the concentration of deferiprone, F_0 is the fluorescence intensity in the absence of deferiprone, and F is the fluorescence intensity at 410 nm in the presence of deferiprone. The calculated limit of detection (LOD) based on $3S_b/m$ (S_b : blank's standard deviation; m : calibration slope) and limit of quantification (LOQ) based on $10 S_b/m$ were 0.003 $\mu\text{g mL}^{-1}$ and 0.01 $\mu\text{g mL}^{-1}$. The precision of the proposed method was evaluated by conducting repeat tests on the same and different days during the investigation. The (RSDs%) for 5 determinations of deferiprone (1.0 $\mu\text{g mL}^{-1}$) were 0.3% and 0.4% for intra-day and inter-day measurements, respectively. The respectable repeatability and reproducibility of the method confirmed the applicability of the nanoprobe for deferiprone monitoring. In order to evaluate the accuracy of the method, known amounts of deferiprone were added to EBC samples and analyzed to determine the recovery rates. As shown in Table 1, the recovery rates for the method ranged from 98 to 104%. A statistical analysis using a t -test confirmed no statistically significant differences between the

Table 2 Robustness study for different levels of deferiprone in different conditions

Condition	RE% for two level of deferiprone ($\mu\text{g mL}^{-1}$)	
	0.1	1.0
One laboratory to another	2.4	1.5
One researcher to another	1	3.5
	2	2.8
	3	3.9

$$\%RE = [(A_{\text{Measured}} - A_{\text{Expected}}) / A_{\text{Expected}}] \times 100$$

Table 3 Comparison of analytical characteristics validated method with other reported techniques in the literature

Method	Sample	LOD ($\mu\text{g mL}^{-1}$)	Linear range ($\mu\text{g mL}^{-1}$)	Reference
Capillary electrophoresis-frontal analysis (CE/FA)	Aqueous solution	1.0	5.5–33.3	[4]
RP-HPLC	Pharmaceutical dosage form	0.21	60–140	[35]
LC-MS/MS	Plasma	0.05	0.1–20	[36]
Flame Atomic Absorption Spectroscopy (FAAS)	Pharmaceuticals, water and food samples	0.032	0.05–3.0	[33]
Spectrophotometry	EBC	0.012	0.05–4.0	[9]
Potentiometry	Bulk and Tablet	0.45	1.39–1391.52	[37]
MIL-101/agarose NCH based fluorescence assay	EBC	0.003	0.005–1.5	This work

expected and measured values, thereby validating the method's accuracy and reliability. The method's robustness was evaluated by examining its performance under varying conditions, when transferred between laboratories or analysts. As shown in Table 2, the results indicate that the method exhibits negligible variability, thereby demonstrating its robustness and reliability. The analytical comparison of the validated method with other reported techniques in literature for the determination of deferiprone was given in Table 3. As can be seen, the current work exhibited comparable sensitivity compared with other systems.

Real samples analysis

To evaluate the analytical applicability and feasibility of the proposed MIL-101/agarose NCH, deferiprone determination was carried out in four EBC samples collected from patients receiving deferiprone. Table 4 presents the findings of the real sample analysis. Recovery experiments were completed by spiking to the concentration of deferiprone (0.05 and 0.5 $\mu\text{g mL}^{-1}$) to confirm the accuracy of the reported values for real sample analyses and study the no interference of other co-administered drugs.

Table 4 Determination of deferiprone in real EBC samples by validated method

No.	Gender	Age (year)	Co-administrated drugs	Added ($\mu\text{g mL}^{-1}$)	Found ($\mu\text{g mL}^{-1}$)	Recovery (%) ^a
1	Female	66	Losartan, Amlodipine, Trifluoperazine	-	0.114	-
				0.05	0.162	96.0
				0.50	0.624	102.0
2	Female	32	Levetiracetam, Calcium, Vitamin D	-	0.030	-
				0.05	0.077	94.0
				0.50	0.528	99.6
3	Male	43	Sodium valproate	-	0.047	-
				0.05	0.094	94.0
				0.50	0.559	102.4
4	Male	61	Metoprolol, Duloxetine, Aspirin	-	0.077	-
				0.05	0.126	98.0
				0.50	0.587	102.0

^a Recovery (%) = [deferiprone concentration in samples (after spiking – before spiking)/Added] × 100

The results indicate a satisfactory recovery percentage of 94.2–102.3%, demonstrating that this experiment is highly accurate and independent from matrix effects for determining deferiprone in biological matrices such as human EBC.

Conclusion

In this research, a simple and efficient method was used to synthesize MIL-101/agarose nanoparticles, which were then utilized as a probe for the detection of deferiprone in EBC samples. Based on the results, the fluorescence emission of the nanoprobe is gradually quenched by increasing the deferiprone concentration. The quenching in the fluorescence is mainly attributed to the chelation effect of the functional groups in deferiprone and Fe centers in the structure of the nanoprobe. The study found a linear relationship between the intensity and deferiprone concentration within the range of 0.005–1.5 $\mu\text{g mL}^{-1}$ with LOD of 0.003 $\mu\text{g mL}^{-1}$. Furthermore, the method's precision was 0.3% and 0.4% RSDs% for intra-day and inter-day measurements, respectively. Besides, respectable recoveries of 94.2–102.3% in the EBC samples exhibited great potential in practical application. It is worth noting that the MIL-101/agarose NCH probe boasts a number of advantageous properties, including a short response time, simplicity of operation, high sensitivity, and good reliability, which render it a valuable asset for the detection of deferiprone in medical diagnostic settings. Despite the promising results, the presented method has some limitations that could impact its suitability for routine clinical use. Despite its advantages, the method's long-term storage stability of the nanomaterials is a concern, which may affect its reliability and consistency over time. Furthermore, the EBC sampling process is inherently subject to some variability, which may impact the method's reliability in clinical settings. Additionally, biological samples often contain matrix compounds that can significantly affect the sensitivity of optical methods, making it challenging to achieve extremely low LODs,

which can be a significant limitation for the practical application of these probes.

Acknowledgements

This study was approved by the ethics committee at Tabriz University of Medical Sciences.

Author contributions

RM: Investigation, writing – original draft, ZK: Design of the work, writing – original draft, JS: Validation, VJ-G: Interpretation of data, validation, MK: Design the work, ER: Analysis, Conceptualization, Writing—review & editing. AJ: Supervision, Writing—review & editing. All authors read and approved the final manuscript.

Funding

This report is a part of the results of R. Moharami's MSc thesis submitted to the Faculty of Pharmacy, Tabriz University of Medical Sciences, Tabriz, Iran, and supported by Tabriz University of Medical Science under grant number of 73290.

Data availability

The datasets used and/or analysed during the current study are available from the corresponding author on reasonable request.

Declarations

Ethics approval and consent to participate

All sample donors or participants filled out and signed the informed consent of project with ethical code IR.TBZMED.PHARMACY.REC.1402.05. This study was approved by the ethics committee at Tabriz University of Medical Sciences.

Consent for publication

Not applicable.

Competing interests

The authors declare no competing interests.

Received: 26 June 2024 / Accepted: 9 September 2024

Published online: 18 September 2024

References

1. Kontoghiorghe CN, Kontoghiorghe GJ. Efficacy and safety of iron-chelation therapy with deferoxamine, deferiprone, and deferasirox for the treatment of iron-loaded patients with non-transfusion-dependent thalassemia syndromes. *Drug Des Devel Ther.* 2016;10:465–81. <https://doi.org/10.2147/dddt.s79458>.

2. Barman Balfour JA, Foster RH. Deferiprone: a review of its clinical potential in iron overload in β -thalassaemia major and other transfusion-dependent diseases. *Drugs*. 1999;58(3):553–78. <https://doi.org/10.2165/00003495-199958030-00021>.
3. Kontoghiorghes GJ, Eracleous E, Economides C, Kolnagou A. Advances in iron overload therapies. Prospects for effective use of deferiprone (L1), deferoxamine, the new experimental chelators ICL670, GT56-252, L1NALL and their combinations. *Curr Med Chem*. 2005;12(23):2663–81. <https://doi.org/10.2174/092986705774463003>.
4. Asmari M, Abdel-Megied AM, Michalcová L, Glatz Z, El Deeb S. Analytical approaches for the determination of deferiprone and its iron (III) complex: investigation of binding affinity based on liquid chromatography-mass spectrometry (LC-ESI/MS) and capillary electrophoresis-frontal analysis (CE/FA). *Microchem J*. 2020;154:104556. <https://doi.org/10.1016/j.microc.2019.104556>.
5. Farokhi S, Roushani M, Hosseini H, Zalpour N, Soleiman-Beigi M. Synthesis of a new nanocomposite based on natural asphalt and its application as a high-performance and eco-friendly platform for the electrochemical determination of deferiprone. *Electrocatalysis*. 2023;14(5):732–40. <https://doi.org/10.1007/s12678-023-00829-8>.
6. Yadegari H, Jabbari A, Heli H, Moosavi-Movahedi AA, Karimian K, Khodadadi A. Electrocatalytic oxidation of deferiprone and its determination on a carbon nanotube-modified glassy carbon electrode. *Electrochim Acta*. 2008;53(6):2907–16. <https://doi.org/10.1016/j.electacta.2007.11.003>.
7. Abbas M, Nawaz R, Iqbal T, Alim M, Asi MR. Quantitative determination of deferiprone in human plasma by reverse phase high performance liquid chromatography and its application to pharmacokinetic study. *Pak J Pharm Sci*. 2012;25(2):343–8.
8. Ubale S, Bhosale M, Parajne SK. Development and validation of RP-HPLC method for estimation of deferiprone and its related impurity in pharmaceutical dosage form. *Asian J Pharm Anal*. 2023;13(1):1–6. <https://doi.org/10.52711/2231-5675.2023.00001>.
9. Sefid-Sefidehkhani Y, Mokhtari M, Jouyban A, Khoubnasabjafari M, Jouyban-Gharamaleki V, Rahimpour E. Utilizing Fe (III)-doped carbon quantum dots as a nanoprobe for deferiprone determination in exhaled breath condensate. *Chem Pap*. 2023;77(3):1445–53. <https://doi.org/10.1007/s11696-022-02563-9>.
10. Akgönüllü S, Denizli A. Recent advances in optical biosensing approaches for biomarkers detection. *Biosens Bioelectron*. 2022;12:100269. <https://doi.org/10.1016/j.biosx.2022.100269>.
11. Elsonbaty A, Hasan MA, Eissa MS, Hassan WS, Abdulwahab S. Synchronous spectrofluorimetry coupled with third-order derivative signal processing for the simultaneous quantitation of telmisartan and chlorthalidone drug combination in human plasma. *J Fluoresc*. 2021;31(1):97–106. <https://doi.org/10.1007/s10895-020-02639-3>.
12. Elsonbaty A, Madkour AW, Abdel-Raouf AM, Abdel-Monem AH, El-Attar AAMM. Computational design for eco-friendly visible spectrophotometric platform used for the assay of the antiviral agent in pharmaceutical dosage form. *Spectrochim Acta Mol Biomol Spectrosc*. 2022;271:120897. <https://doi.org/10.1016/j.saa.2022.120897>.
13. Vaitis C, Sourkouni G, Argiris C. Metal organic frameworks (MOFs) and ultrasound: a review. *Ultrason Sonochem*. 2019;52:106–19. <https://doi.org/10.1016/j.ultrsonch.2018.11.004>.
14. Mohan B, Virender, Gupta RK, Pombeiro AJ, Solovev AA, Singh G. Advancements in metal-organic, enzymatic, and nanocomposite platforms for wireless sensors of the next generation. *Adv Funct Mater*. 2024. <https://doi.org/10.1002/adfm.202405231>.
15. Cao J, Li X, Tian H. Metal-organic framework (MOF)-based drug delivery. *Curr Med Chem*. 2020;27(35):5949–69. <https://doi.org/10.2174/0929867326666190618152518>.
16. Mohan B, Kumar S, Chen Q. Obtaining water from air using porous metal-organic frameworks (MOFs). *Top Curr Chem*. 2022;380(6):54. <https://doi.org/10.1007/s41061-022-00410-9>.
17. Furukawa H, Cordova KE, O'Keeffe M, Yaghi OM. The chemistry and applications of metal-organic frameworks. *Science*. 2013;341(6149):1230444. <https://doi.org/10.1126/science.1230444>.
18. Mohan B, Priyanka, Singh G, Chauhan A, Pombeiro AJL, Ren P. Metal-organic frameworks (MOFs) based luminescent and electrochemical sensors for food contaminant detection. *J Hazard Mater*. 2023;453:131324. <https://doi.org/10.1016/j.jhazmat.2023.131324>.
19. Zhang H, Hu X, Li T, Zhang Y, Xu H, Sun Y, Gu X, Gu C, Luo J, Gao B. MIL series of metal organic frameworks (MOFs) as novel adsorbents for heavy metals in water: a review. *J Hazard Mater*. 2022;429:128271. <https://doi.org/10.1016/j.jhazmat.2022.128271>.
20. Keshta BE, Yu H, Wang L. MIL series-based MOFs as effective adsorbents for removing hazardous organic pollutants from water. *Sep Purif Technol*. 2023;322:124301. <https://doi.org/10.1016/j.seppur.2023.124301>.
21. Kitao T, Zhang Y, Kitagawa S, Wang B, Uemura T. Hybridization of MOFs and polymers. *Chem Soc Rev*. 2017;46(11):3108–33. <https://doi.org/10.1039/c7cs00041c>.
22. Sun W, Zhao X, Webb E, Xu G, Zhang W, Wang Y. Advances in metal-organic framework-based hydrogel materials: preparation, properties and applications. *J Mater Chem A*. 2023;11:2092–127. <https://doi.org/10.1039/D2TA08841J>.
23. Ahmed EM. Hydrogel. Preparation, characterization, and applications: a review. *J Adv Res*. 2015;6(2):105–. <https://doi.org/10.1016/j.jare.2013.07.006>.
24. Sanagi MM, Loh SH, Wan Ibrahim WN, Pourmand N, Salisu A, Wan Ibrahim WA, Ali I. Agarose-and alginate-based biopolymers for sample preparation: excellent green extraction tools for this century. *J Sep Sci*. 2016;39(6):1152–59. <https://doi.org/10.1002/jssc.201501207>.
25. Hu H, Zhang H, Chen Y, Chen Y, Zhuang L, Ou H. Enhanced photocatalysis degradation of organophosphorus flame retardant using MIL-101 (Fe)/per-sulfate: effect of irradiation wavelength and real water matrixes. *Chem Eng J*. 2019;368:273–84. <https://doi.org/10.1016/j.cej.2019.02.190>.
26. Karimzadeh Z, Gharekhan A, Rahimpour A, Jouyban A. Dual-emission ratiometric fluorescent probe based on N-doped CQDs@UiO-66/PVA nanocomposite hydrogel for quantification of pethidine in human plasma. *Mikrochim Acta*. 2023;190(4):128. <https://doi.org/10.1007/s00604-023-05703-4>.
27. Khoubnasabjafari M, Jouyban-Gharamaleki V, Ghanbari R, Jouyban A. Exhaled breath condensate as a potential specimen for diagnosing COVID-19. *Bio-analysis*. 2020;12(17):1195–97. <https://doi.org/10.4155/bio-2020-0083>.
28. Mohan B, Tao Z, Kumar S, Xing T, Ma S, Huang W, Yang X, You H, Ren P. Water- and pH-stable methylthio-containing metal-organic frameworks as luminescent sensors for metal-ion detection. *Cryst Growth Des*. 2022;22(9):5407–15. <https://doi.org/10.1021/acs.cgd.2c00493>.
29. Ghasemzadeh H, Afraz S, Moradi M, Hassanpour S. Antimicrobial chitosan-agarose full polysaccharide silver nanocomposite films. *Int J Biol Macromol*. 2021;15:179532–41. <https://doi.org/10.1016/j.jbiomac.2021.02.192>.
30. Liu Z, He W, Zhang Q, Shapour H, Bakhtari MF. Preparation of a GO/MIL-101 (Fe) composite for the removal of methyl orange from aqueous solution. *ACS Omega*. 2021;6(7):4597–608. <https://doi.org/10.1021/acsomega.0c05091>.
31. Kumar N, Desagani D, Chandran G, Ghosh NN, Karthikeyan G, Waigaonkar S, Ganguly A. Biocompatible agarose-chitosan coated silver nanoparticle composite for soft tissue engineering applications. *Artif Cells Nanomed Biotechnol*. 2018;46(3):637–49. <https://doi.org/10.1080/21691401.2017.1337021>.
32. Mohan B, Kumar S, Ma S, You H, Ren P. Mechanistic insight into charge and energy transfers of luminescent metal-organic frameworks based sensors for toxic chemicals. *Adv Sustain Syst*. 2021;5(5):2000293. <https://doi.org/10.1002/advsu.202000293>.
33. Pragourpun K, Sakee U, Fernandez C, Kruanetr S. Deferiprone, a non-toxic reagent for determination of iron in samples via sequential injection analysis. *Spectrochim Acta Mol Biomol Spectrosc*. 2015;142:110–17. <https://doi.org/10.1016/j.saa.2015.01.081>.
34. Tam TF, Leung-Toung R, Wang Y, Zhao Y, Xin T, Shah B, N'zema B, Wodzinska JM, Premyslova M. Fluorinated derivatives of 3-hydroxypyridin-4-ones. *United States Pat*. 2015;EP2448922A1.
35. Sutar S, Patil P, Marchande D, Patil S, Sandgar S, Kumbhar R. RP-HPLC method development for simultaneous estimation of oral iron chelator deferiprone and its related impurity. *Res J Pharm Technol*. 2023;16(4):1890–94. <https://doi.org/10.52711/0974-360X.2023.00310>.
36. Song TS, Hsieh YW, Peng CT, Liu CH, Chen TL, Hour MJ. Development of a fast LC-MS/MS assay for the determination of deferiprone in human plasma and application to pharmacokinetics. *Biomed Chromatogr*. 2012;26(12):1575–81. <https://doi.org/10.1002/bmc.2734>.
37. Kam A, Nm E. Electrochemical determination of deferiprone using PVC membrane sensors. *Austin J Anal Pharm Chem*. 2018;5(1):1098.

Publisher's note

Springer Nature remains neutral with regard to jurisdictional claims in published maps and institutional affiliations.